Finite-Element Analysis of Temperature Increase in Vascularized Biological Tissues Exposed to RF Sources

V. De Santis[1], M. Feliziani[1], F. Maradei[2], and C. Buccella[1]

[1]Department of Electrical and Computer Engineering, University of L'Aquila, 67100 L'Aquila, Italy
[2]Department of Electrical Engineering, Sapienza University of Rome, 00185 Rome, Italy

A new model of numerical dosimetry is proposed for RF exposure. First, the specific absorption rate (SAR) is computed. Then, the heat transfer governed by the bio-heat equation with convection term is numerically solved by a finite-element method (FEM) procedure considering the discrete vascular model of the perfused tissue. By some manipulations of the FEM equations and by generating an adequate FEM mesh, it is possible to solve the thermal convection in the blood vessels considering a one-dimensional domain embedded in the fully three-dimensional domain where only the thermal diffusion is analyzed.

***Index Terms*—Bio-heat equation, discrete vascular model, finite-element method (FEM), numerical dosimetry.**

I. Introduction

RECENTLY, the wide use of wireless applications with the obvious consequence of electromagnetic field (EMF) human exposure, and the possibility to use EMF in medical applications for therapy and diagnostics, have given a pulse to the research in the electrothermal interaction between the aforementioned fields and biological tissues. The relevant part of this topic is addressed to the study of the numerical dosimetry [1], which consists mostly in the evaluation of the temperature increase in tissues exposed to high-frequency EM fields.

Mainly, the models of heat transfer in perfused tissues can be divided into two classes: continuum models and discrete vascular models. The continuum models are the most popular and easy to implement, but they are unable to predict the significant thermal effects of vessels on the local tissue temperature [2]. To overcome this inconvenience, some models of discrete vasculature have been recently proposed to take into account the presence of veins and arteries by finite difference procedures [3], [4].

To improve the actual models of discrete vasculature, a new method, based on the finite-element method (FEM) solution of the electrothermal problem considering diffusion and convection in a 3-D domain, is proposed.

II. Mathematical Formulation

The transient convection-diffusion problem is described by the linear operator $L(T)$

$$L(T) = \rho c\left(\frac{\partial T}{\partial t} + \boldsymbol{v}\cdot\nabla T\right) - \nabla\cdot k\nabla T - \rho\mathrm{SAR} - A = 0 \tag{1}$$

where T is the unknown temperature, ρ the mass density, c the specific heat, k the thermal conductivity, $\boldsymbol{v}$ the velocity field, A the metabolic rate, and SAR the specific absorption rate due to electromagnetic sources. It should be noted that the SAR must be known before solution of (1). It can be calculated by solving the electromagnetic field problem of the RF exposure [1].

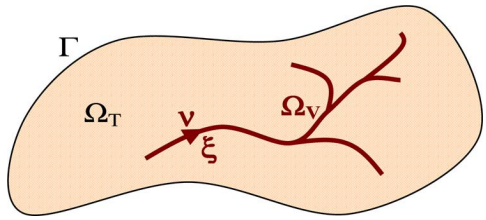

Fig. 1. Vascular structure embedded in a tissue.

The solution of the convection-diffusion problem (1) in a bounded domain Ω delimited by the boundary Γ requires the boundary conditions

$$T - T_D = 0 \quad \text{on } \Gamma_\mathrm{D} \tag{2a}$$

$$k\frac{\partial T}{\partial n} + q + h(T - T_N) = 0 \quad \text{on } \Gamma_\mathrm{N} \tag{2b}$$

where Γ_D and Γ_N denote Dirichlet and Neumann boundaries, and $\Gamma = \Gamma_\mathrm{D} + \Gamma_\mathrm{N}$, q is a known heat flow, h is the heat transfer coefficient, T_D and T_N are known temperatures on Γ_D and Γ_N, respectively.

Equations (1) with (2) could be solved by any numerical method based on partial differential equation (PDE) solution, but the standard FEM solution of a highly vascularized domain requires the fine discretization of vessels into 3-D elements, leading to a huge number of unknowns and therefore making the numerical solution quite impracticable. In order to reduce the degrees of freedom (DoF), a new model is proposed.

The computational domain Ω related to a vascularized tissue is divided into two subregions ($\Omega = \Omega_\mathrm{V} + \Omega_\mathrm{T}$): Ω_V is the region of the vascular system where the blood flows, and Ω_T is the tissue region where the vascular system is embedded, as shown in Fig. 1.

Applying the standard Galerkin method it yields

$$\int_\Omega N_i L(T)d\Omega = \int_{\Omega_\mathrm{T}} N_i L(T)d\Omega + \int_{\Omega_\mathrm{V}} N_i L(T)d\Omega = 0 \tag{3}$$

where N_i is the weighting function.

Manuscript received October 07, 2008. Current version published February 19, 2009.Corresponding author: V. De Santis (e-mail: desantis.valerio@ing.univaq.it).

Color versions of one or more of the figures in this paper are available online at http://ieeexplore.ieee.org.

Digital Object Identifier 10.1109/TMAG.2009.2012781

The Galerkin form of the linear operator $L(T)$ in Ω_{T}, where there is no blood flow and therefore $\boldsymbol{v}=0$, is given by

$$\int_{\Omega_{\mathrm{T}}} N_i L(T)d\Omega = \int_{\Omega_{\mathrm{T}}} N_i \left(\rho c\frac{\partial T}{\partial t} - \nabla\cdot k\nabla T - \rho\mathrm{SAR} - A\right) d\Omega = 0 \tag{4}$$

and in Ω_{V} by

$$\int_{\Omega_V} N_i L(T)d\Omega = \int_{\Omega_V} N_i \left[\rho_b c_b\left(\frac{\partial T}{\partial t} + \boldsymbol{v}\cdot\nabla T\right) - \nabla\cdot k_b\nabla T - \rho_b\mathrm{SAR} - A\right] d\Omega = 0 \tag{5}$$

where ρ_b, c_b and k_b are the specific constants of blood.

Assuming a vessel with small cross section dimension respect to the other physical dimensions, the 3-D domain Ω_{V} can be modeled by the thin vessel approximation assuming $d\Omega = S_V d\xi$ with ξ the one-dimensional curvilinear coordinate of the vessel (see Fig. 1), and S_V its cross section area. By this assumption (5) becomes

$$\int_{\Omega_V} N_i L(T)d\Omega = \int_{\ell_\xi} S_V N_i \left[\rho_b c_b\left(\frac{\partial T}{\partial t} + \boldsymbol{v}\cdot\nabla T\right) - \nabla\cdot k_b\nabla T - \rho_b\mathrm{SAR} - A\right] d\xi = 0 \tag{6}$$

where ℓ_ξ is the vessel length. Equation (6) can be simplified by the following assumptions:

- — the vessel cross section S_V is constant inside the discretized vessel segment;
- — the direction of the velocity $\boldsymbol{v}$ is always tangent to the vessel abscissa ξ;
- — the temperature in the vessel cross section is constant, and therefore the conduction coefficient of the blood, k_b, is nonzero only in the direction of the flow;
- — the SAR and the metabolic rate A are negligible due to the thin vessel approximation.

Equation (6) is then reduced to

$$\int_{\Omega_V} N_i L(T)d\Omega \approx S_V\int_{\ell_\xi} N_i\left[\rho_b c_b\left(\frac{\partial T}{\partial t} + v\frac{\partial T}{\partial \xi}\right) - \frac{\partial}{\partial\xi}k_b\frac{\partial T}{\partial\xi}\right] d\xi = 0 \tag{7}$$

where the blood velocity v is assumed to be a scalar quantity.

Both (4) and (7) can be solved by the finite-element method adopting a suitable mesh, and the two solution systems are assembled together as described in details in the following sections.

A. 3-D Finite-Element Solution of Conduction Equation

The solution of the diffusion equation (4) is straightforward by applying the standard Galerkin finite-element procedure [5], [6]. The local equation in a 3-D finite-element $\Omega_{\mathrm{T}}^{(\mathrm{e})}$ is given by

$$\int_{\Omega_{\mathrm{T}}^{(\mathrm{e})}} \rho c N_i\frac{\partial T}{\partial t}d\Omega - \int_{\Omega_T^{(e)}} N_i\nabla\cdot k\nabla T d\Omega - \int_{\Omega_{\mathrm{T}}^{(\mathrm{e})}} N_i(\rho\mathrm{SAR} + A)d\Omega = 0. \tag{8}$$

By applying first Green's theorem, the second integral in (8) becomes

$$\int_{\Omega_{\mathrm{T}}^{(\mathrm{e})}} \rho c N_i\frac{\partial T}{\partial t}d\Omega + \int_{\Omega_{\mathrm{T}}^{(\mathrm{e})}} k\nabla N_i\cdot\nabla T d\Omega - \int_{\Gamma_{\mathrm{T}}^{(\mathrm{e})}} kN_i\frac{\partial T}{\partial n}d\Gamma - \int_{\Omega_{\mathrm{T}}^{(\mathrm{e})}} N_i(\rho\mathrm{SAR} + A)d\Omega = 0 \tag{9}$$

where $\Gamma_{\mathrm{T}}^{(\mathrm{e})}$ is the element boundary of $\Omega_{\mathrm{T}}^{(\mathrm{e})}$ and n is the direction normal to the boundary. Note that in the assembling process the boundary terms for adjacent elements simplifies, so their contribution is nonzero only on the computational domain boundaries [5].

The temperature T is approximated at any point inside the finite-element $\Omega_{\mathrm{T}}^{(\mathrm{e})}$ by the nodal based FEM expansions as

$$T(x,y,z) = \sum_{j=1}^{m} N_j(x,y,z)T_j \tag{10}$$

where m is the number of element nodes, T_j are the temperature nodal values, $N_j(x,y,z)$ is the 3-D nodal interpolating function associated to the jth node and equal to the weighting function [5], [6].

Equation (9) can be rewritten in compact form as

$$[M_T]\frac{\partial[T]}{\partial t} + [K_T][T] = [F_T] \tag{11}$$

where $[T] = [T_1\, T_2 \ldots T_m]^t$ is the vector containing the temperature of the element nodes, and the coefficients $(i,j = 1,2,\ldots,m)$ of the FEM local matrices in tissues are given by

$$M_{T_{ij}} = \int_{\Omega_{\mathrm{T}}^{(\mathrm{e})}} \rho c N_i N_j d\Omega \tag{12a}$$

$$K_{T_{ij}} = \int_{\Omega_{\mathrm{T}}^{(\mathrm{e})}} k\nabla N_i\cdot\nabla N_j d\Omega + \int_{\Gamma_{\mathrm{T}}^{(\mathrm{e})}} hN_iN_j d\Gamma \tag{12b}$$

$$F_{T_i} = \int_{\Omega_{\mathrm{T}}^{(\mathrm{e})}} N_i(\rho\mathrm{SAR} + A)d\Omega - \int_{\Gamma_{\mathrm{T}}^{(\mathrm{e})}} N_i(q - hT_N)d\Gamma. \tag{12c}$$

B. 1-D Finite-Element Solution of Convection-Diffusion Equation

The temperature in a 1-D linear element between nodes i and j having length Δ_{ij} is approximated by

$$T(\xi) = N_i(\xi)T_i + N_j(\xi)T_j = [N]^t[T] \tag{13}$$

where $[N]^t = [N_i(\xi)\ N_j(\xi)]$ is the vector of the 1-D linear shape functions, and $[T] = [T_i\ T_j]^t$. The Galerkin local form of (7) in matrix form is given via (13) by

$$S_V \int_{\Delta_{ij}} \rho_b c_b [N][N]^t \frac{\partial [T]}{\partial t} d\xi + v S_V \int_{\Delta_{ij}} \rho_b c_b [N] \frac{\partial [N]^t}{\partial \xi} [T] d\xi - S_V \int_{\Delta_{ij}} [N] \frac{\partial}{\partial \xi} k_b \frac{\partial [N]^t}{\partial \xi} [T] d\xi = 0 \quad (14)$$

assuming v to be constant inside the element Δ_{ij}.

By applying Green's theorem to the last integral in (14) we obtain

$$S_V \int_{\Delta_{ij}} \rho_b c_b [N][N]^t \frac{\partial [T]}{\partial t} d\xi + v S_V \int_{\Delta_{ij}} \rho_b c_b [N] \frac{\partial [N]^t}{\partial \xi} [T] d\xi + S_V \int_{\Delta_{ij}} k_b \frac{\partial [N]}{\partial \xi} \frac{\partial [N]^t}{\partial \xi} [T] d\xi - S_V \int_{\Gamma_V^{(e)}} k_b [N] \frac{\partial [N]^t}{\partial \xi} [T] d\Gamma = 0. \quad (15)$$

The above equation can be written in local compact form as

$$[M_V] \frac{\partial [T]}{\partial t} + [C_V][T] + [K_V][T] = [F_V] \quad (16)$$

where the local matrix coefficients are given by

$$M_{V_{ij}} = S_V \int_{\Delta_{ij}} \rho_b c_b N_i N_j d\xi \quad (17a)$$

$$C_{V_{ij}} = v S_V \int_{\Delta_{ij}} \rho_b c_b N_i \frac{\partial N_j}{\partial \xi} d\xi \quad (17b)$$

$$K_{V_{ij}} = S_V \int_{\Delta_{ij}} k_b \frac{\partial N_i}{\partial \xi} \frac{\partial N_j}{\partial \xi} d\xi + \int_{\Gamma_V^{(e)}} h N_i N_j d\Gamma \quad (17c)$$

$$F_{V_i} = \int_{\Gamma_V^{(e)}} N_i (h T_N - q) d\Gamma. \quad (17d)$$

C. Global Finite-Element Solution System

Solution of (3) can be carried out by using the Crank–Nicholson scheme for time integration. It means that the time derivative in (11) and (16) can be approximated at time instant $t = (n + 1/2)\Delta t$ by

$$\frac{\partial [T]}{\partial t} \approx \frac{[T]^{n+1} - [T]^n}{\Delta t}. \quad (18)$$

At this point, it is necessary that the 1-D elements of the vessels must coincide with some edges of the 3-D finite elements, so that the nodes of the 1-D structure are also nodes of the 3-D FEM mesh, as schematically shown in Fig. 2. By this assumption, it is therefore possible to assemble the local matrices of the three-dimensional elements used to discretize the region Ω_T

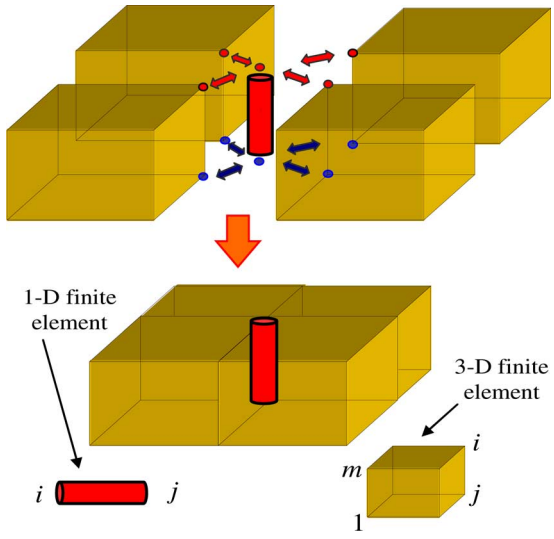

Fig. 2. 1-D vessel element embedded in the 3-D tissue domain.

with the local matrices of the 1-D elements used for the Ω_V region, and the final equation system is obtained

$$[M] \frac{[T]^{n+1} - [T]^n}{\Delta t} + ([C] + [K]) \frac{[T]^{n+1} + [T]^n}{2} = \frac{[F]^{n+1} + [F]^n}{2} \quad (19)$$

where the global FEM matrices are given by

$$[M] = [M_V] + [M_T] \quad (20a)$$

$$[C] = [C_V] \quad (20b)$$

$$[K] = [K_V] + [K_T] \quad (20c)$$

$$[F] = [F_V] + [F_T]. \quad (20d)$$

If standard Galerkin method is applied to solve the convection-diffusion equation, the results should be affected by spurious oscillation in space due to the discretization of the convection transport term. This occurs when certain parameters exceed a critical value (i.e., element Peclet number $P_e = \rho c v \Delta_x / (2k)$, with Δ_x the finite-element size). Therefore, it can be necessary to add to (19) some stabilization matrices applying the Characteristic Galerkin (GC) method as described in [7].

III. Applications

First, the proposed model has been validated in a very simple test case by comparing the obtained results with those obtained by a commercial software tool (Comsol Multi-Physics) with a fully 3-D mesh (i.e., 3-D discretization also inside vessel). The considered configuration is composed by a cylindrical vessel embedded in a cylindrical tissue region as shown in Fig. 3(a). Assuming for the tissue $\rho = 1000$ kg/m^3, $c = 3200$ J/(kg°C), $k = 0.5$ W/(m°C), $A = 0, \mathrm{SAR} = 0$, and for the blood $\rho_b = 1060$ kg/m^3, $c_b = 3600$ J/(kg°C), $k_b = 0.6$ W/(m°C), $v = 0.02$ m/s, the obtained temperature profiles along the vessel axis are reported in Fig. 3(b). It should be observed that the good agreement between the different approaches confirms the validity of the proposed method.

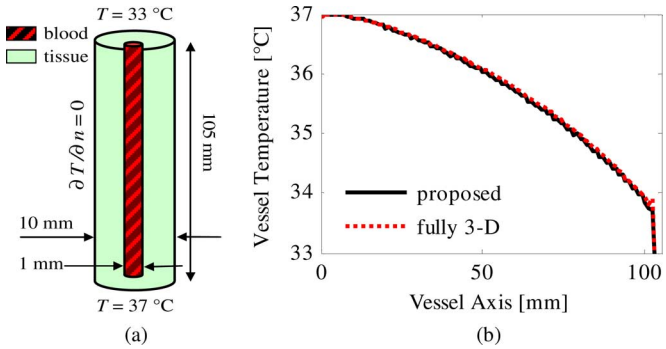

Fig. 3. (a) Test case configuration and (b) numerical results.

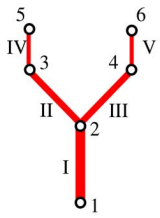

	Δ_{ij} [cm]	r [mm]	v [m/s]
I	2.0	0.5	0.02
II	1.8	0.3	0.028
III	1.8	0.3	0.028
IV	1.0	0.2	0.025
V	1.0	0.2	0.025

(b)

Fig. 4. (a) Vascular structure and (b) related properties.

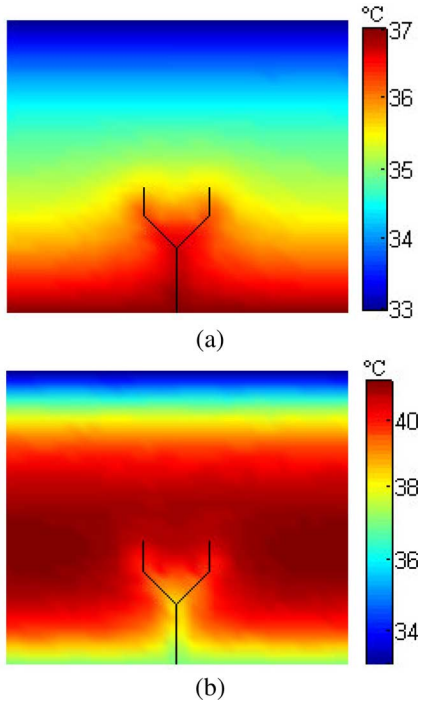

Fig. 5. (a) Normo-thermal temperature distribution ($\mathrm{SAR} = 0$). (b) Temperature distribution for $\mathrm{SAR} = 10$ W/kg.

Then, a vessel structure with bifurcations and bends is considered as reported in Fig. 4(a). The related physical properties (i.e., length, radius, and velocity of the vessel segments) are shown in Fig. 4(b). The vasculature is assumed to be embedded in a cubic region of tissue with dimension $10 \times 10 \times 10$ cm. On the top and bottom facets of the cubic region, Dirichlet essential type boundary conditions have been applied ($T_D = 37$ °C on top, $T_D = 33$ °C on bottom); on the other facets Neumann natural boundary conditions occur.

The maps of temperature distributions, assuming $\mathrm{SAR} = 0$ (i.e., normo-thermal temperature distribution) and $\mathrm{SAR} = 10$ W/kg (i.e., intense exposition) are reported in Fig. 5(a) and (b), respectively. For the sake of simplicity the SAR has been considered spatially constant in the proposed applications, but it can be obviously considered with a nonuniform distribution and easily calculated [1]. From this figure it is evident the cooling/warming effect of the large vessels on the tissue temperature profile. In other words, the thermoregulatory mechanism of the blood flow is well modeled.

IV. Conclusion

A novel numerical model has been proposed to evaluate the temperature increase in a RF exposed biological tissue with discrete vascularization. The model has been developed using the finite-element formulation. Using the thin vessel approximation, the arteries have been modeled by 1-D finite elements embedded in the tissue region that has been discretized in 3-D finite elements. By generating an adequate mesh, it is possible to reduce dramatically the computational cost. The proposed procedure can be very useful to predict the thermal distribution inside human body with higher accuracy than that of the methods based on the traditional continuum model. Therefore, possible applications of the proposed method are related to RF thermal dosimetry for safety standards and biomedical applications as hyperthermia cancer treatment.

References

[1] C. Buccella, V. De Santis, and M. Feliziani, "Prediction of temperature increase in human eyes due to RF sources," *IEEE Trans. Electromag. Compat.*, vol. 49, no. 4, pp. 825–833, Nov. 2007.

[2] H. H. Pennes, "Analysis of tissue and arterial blood temperature in resting forearm," *J. Appl. Phys.*, vol. 1, pp. 93–122, 1948.

[3] A. N. T. J. Kotte, G. M. J. Van Leeuwen, and J. J. W. Lagendijk, "Modelling the thermal impact of a discrete vessel tree," *Phys. Med. Biol.*, vol. 44, pp. 57–74, 1999.

[4] M. Stańczyk, G. M. J. Van Leeuwen, and A. A. Van Steenhoven, "Discrete vessel heat transfer in perfused tissue—Model comparison," *Phys. Med. Biol.*, vol. 52, pp. 2379–2391, 2007.

[5] R. W. Lewis, P. Nithiarasu, and K. N. Seetharamu, *Fundamentals of the Finite Element Method for Heat and Fluid Flow*. Chichester, U.K.: Wiley, 2004.

[6] O. C. Zienkievich and L. R. Taylor, "The Basis," in *The Finite Element Method*. Oxford, U.K.: Butterworth-Heinemann, 2000, vol. 1.

[7] O. C. Zienkievich and L. R. Taylor, "Fluid Dynamics," in *The Finite Element Method*. Oxford, U.K.: Butterworth-Heinemann, 2000, vol. 3.